ELECTROWEAK MEASUREMENTS FROM RUN II AT THE TEVATRON

T. R. WYATT

Department of Physics and Astronomy, University of Manchester, Manchester M13 9PL, UK
Email: twyatt@fnal.gov

The CDF and DØ detectors were fully commissioned for physics running in Run II at the Tevatron $p\bar{p}$ collider in early 2002. Since then both experiments have collected data samples corresponding to an integrated luminosity of around $\int L = 200$ pb^{-1} at a $p\bar{p}$ centre-of-mass energy of $\sqrt{s} = 1.96$ TeV. Datasets corresponding $\int L = 120$ pb^{-1} have been analyzed for physics so far. Recent electroweak measurements from Run II are reviewed. Cross section times branching ratio measurements ($\sigma \cdot \mathrm{Br}$) are presented for the intermediate vector bosons (IVB's) in their leptonic decay modes: $W \to \ell\nu$ and $Z \to \ell^+\ell^-$. For the first time, a combination of the $\sigma \cdot \mathrm{Br}$ results from the CDF and DØ experiments is made; this includes using a consistent choice of the total inelastic $p\bar{p}$ cross section for the luminosity determinations of the two experiments. Quantities derived from these $\sigma \cdot \mathrm{Br}$ values are also updated. These include: R_ℓ the ratio of the $\sigma \cdot \mathrm{Br}$ values for W and Z; $\mathrm{Br}(W \to \ell\nu)$, the leptonic branching ratio of the W; and Γ_W, the total decay width of the W. Other measurements using events containing W and Z leptonic decays are presented, including studies that probe the QCD phenomenology of W/Z production and searches for events containing two intermediate vector bosons.

1. Experimental Measurements of $\sigma \cdot \mathrm{Br}$ for $Z \to \ell^+\ell^-$ and $W \to \ell\nu$

1.1. *Introduction*

Figure 1 shows the mechanism for IVB production in $p\bar{p}$ collisions.

The experimental signature for $Z \to \ell^+\ell^-$ is illustrated in Fig. 2. We observe a pair of oppositely charged leptons that have high p_T with respect to the beam direction and are isolated with respect to other energetic particles in the event. The presence of two high p_T leptons in the event leads to a high degree of redundancy in the trigger and offline selection. This leads to low backgrounds and excellent control of systematic uncertainties.

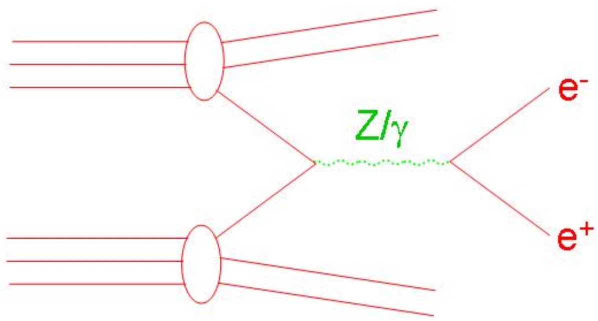

Figure 1. The mechanism for IVB production in $p\bar{p}$ collisions.

The experimental signature for $W \to \ell\nu$ is illustrated in Fig. 3. We observe a single high p_T isolated charged lepton plus missing transverse momentum, $\mathrm{E}_\mathrm{T}^\mathrm{miss}$, carried away by the unobserved neutrino. The

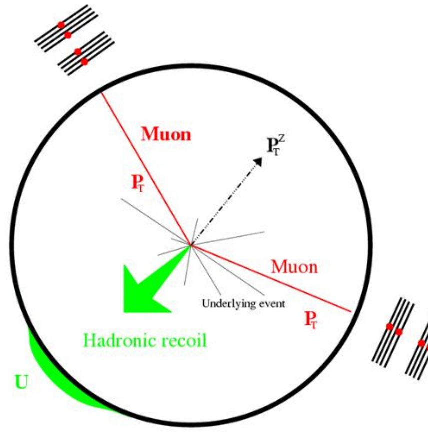

Figure 2. An illustration of the experimental signature for $Z \to \ell^+\ell^-$ in $p\bar{p}$ collisions.

presence of only one high p_T lepton in $W \to \ell\nu$ events leads to less redundancy in the trigger and offline selection than for $Z \to \ell^+\ell^-$. In addition, the measurement of $\mathrm{E}_\mathrm{T}^\mathrm{miss}$ requires us to understand the measurement of the p_T of the hadrons recoiling against the W. These issues make it more difficult to control backgrounds and systematic uncertainties in the analysis of W's than is the case for Z's. Of course, from the point of view of electroweak physics, measurements at the Tevatron on W's are much more interesting than those on Z's, since the properties of the Z have been so well understood at LEP and SLC. However, the samples of Z events are extremely useful as a means to measure experimental efficiencies and control phenomenological systematic uncer-

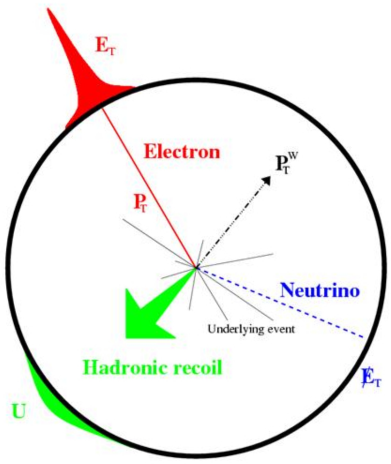

Figure 3. An illustration of the experimental signature for $W \to \ell\nu$ in $p\bar{p}$ collisions.

tainties. Most experimental systematics currently quoted are limited by the size of the data samples currently available and will decrease as larger data samples are collected and analyzed.

In measuring the rate of production of W and Z events at the Tevatron the dominant systematic error arises from the determination of the $p\bar{p}$ luminosity. For CDF this uncertainty is quoted at 6% and for DØ it is quoted as 10% for the preliminary results presented so far. These respective uncertainties are, of course, completely correlated amongst all of the measurements made by an individual experiment. A large part of the above uncertainties is correlated between the two experiments. The treatment of the luminosity scale and uncertainties for the purposes of combining the CDF and DØ results will be discussed in Sec. 2.1.

The other significant source of systematic uncertainty that introduces correlations among the measurements arises from uncertainties in the parton distribution functions (PDF's). Experimentally the observed charged leptons from IVB decay are required to lie within a given range of pseudorapidity (η). The probability for the leptons to lie within this acceptance depends on the degree to which the IVB's are boosted along the beam direction, and this in turn depends on the PDF's. Accurate knowledge of the PDF's is therefore essential in order to determine the experimental acceptance. Of equal importance, a quantitative assessment of the uncertainties in the PDF's is essential in order to evaluate the resulting uncertainty in the experimental acceptance. The uncertainties in the $\sigma \cdot \mathrm{Br}$ measurements of both experiments have been evaluated using the PDF error sets provided as part of the CTEQ6 PDF's.[1]

When determining $\sigma \cdot \mathrm{Br}$ for $Z \to \ell^+\ell^-$ it must be borne in mind that the physically observed process is $p\bar{p} \to \ell^+\ell^- X$; the $\ell^+\ell^-$ system may couple to a Z or a γ. In order to determine the (unphysical) quantity $\sigma_{\mathrm{Z}} \cdot \mathrm{Br}(Z \to \ell^+\ell^-)$ the number of observed $\ell^+\ell^-$ events must therefore be "corrected" by the factor $\sigma_Z/\sigma_{Z\gamma}$, where $\sigma_{Z\gamma}$ is the full Standard Model cross section including Z, γ and Z-γ interference, and σ_Z is the cross section calculated using Z exchange only.

1.2. *DØ: $Z \to \mu^+\mu^-$*

The DØ experiment has updated its measurement of $\sigma_{\mathrm{Z}} \cdot \mathrm{Br}(Z \to \mu^+\mu^-)$ for this conference using a dataset corresponding to $\int L = 117\ \mathrm{pb}^{-1}$. The event selection cuts require two oppositely charged central tracks with $p_{\mathrm{T}} > 15$ GeV. In order to maintain a high selection efficiency the tracks are required to satisfy only loose requirements on muon identification and only one of the muons is required to be isolated. Events are selected over a wide angular range $|\eta| < 1.8$ and a loose cut on the invariant mass of the $\mu^+\mu^-$ system, $\mathrm{M}_{\mu\mu} > 30$ GeV, is made. Cosmic ray muons are rejected by cuts on scintillator timing and the distance of closest approach of the muons to the beam crossing point. The invariant mass of the 6126 DØ $\mu^+\mu^-$ candidates is shown in Fig. 4. The dominant backgrounds arise from QCD $(0.6 \pm 0.3)\%$ and $Z \to \tau^+\tau^-$ $(0.5 \pm 0.1)\%$.

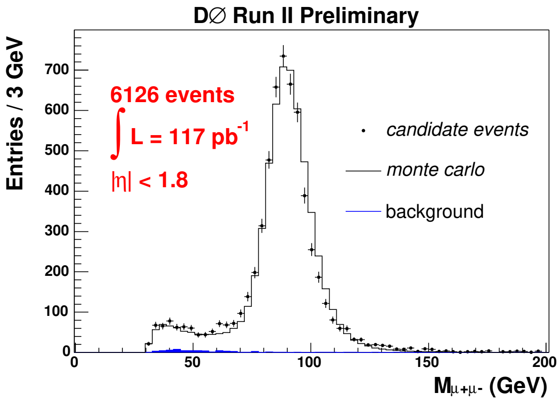

Figure 4. The invariant mass of DØ $\mu^+\mu^-$ candidates.

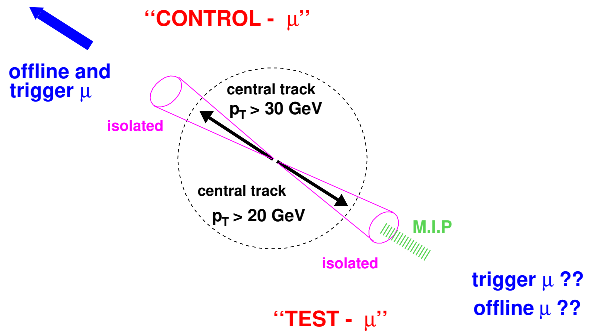

Figure 5. Illustration of the methods used to evaluate experimental efficiencies using the $Z \to \ell^+\ell^-$ data. In this particular figure, the muon trigger efficiency for the "test" muon is evaluated. This measurement uses a pure sample of $Z \to \mu^+\mu^-$ events that is triggered and selected without any bias as to whether or not the "test" muon is detected by the muon system.

An illustration of the methods used to evaluate experimental efficiencies using the $Z \to \ell^+\ell^-$ data is given in Fig. 5. The basic idea is that a very pure sample of $Z \to \mu^+\mu^-$ events can be selected by making rather tight cuts on one "control" muon and only very loose cuts on the second "test" muon. In Fig. 5, the muon trigger efficiency for the "test" muon is evaluated using a sample of $Z \to \mu^+\mu^-$ events that is triggered and selected without any bias as to whether or not the "test" muon is detected by the muon system. In making such measurements it is important to demonstrate that a very pure sample of $Z \to \mu^+\mu^-$ events can be selected even though only loose cuts are made on the "test" muon. This is illustrated by Fig. 6, which shows a comparison of the shapes of the $\mu^+\mu^-$ invariant mass distributions for the two relevant sub-samples of DØ $Z \to \mu^+\mu^-$ events: the points with error bars show the events in which the test muon did not fire the Level-1 trigger; the line histogram shows the events in which the test muon did fire the Level-1 trigger. The shapes of the two distributions are very similar, both being dominated by $Z \to \mu^+\mu^-$. The resulting efficiency per muon of the DØ Level-1 muon trigger as a function of η is shown in Fig. 7. The efficiencies measured in the data for the trigger, tracking and muon identification are used as inputs to a Monte Carlo simulation that is used to evaluate the overall event acceptance $\times$ efficiency. The total acceptance $\times$ efficiency for a $Z \to \mu^+\mu^-$ event to be triggered and selected is 19%.

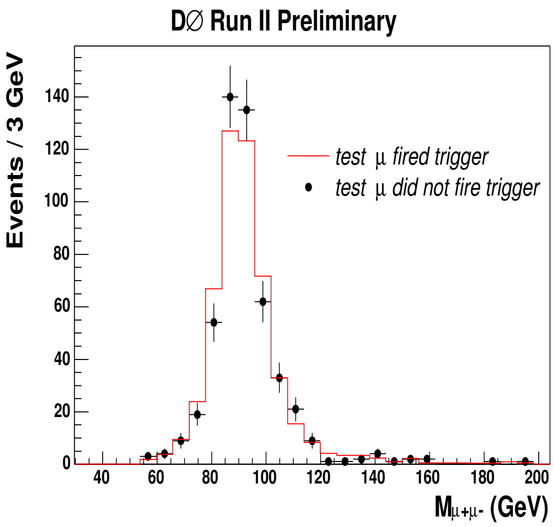

Figure 6. Comparison of the shapes of the invariant mass distributions for two samples of DØ $Z \to \mu^+\mu^-$ events: *points with error bars:* test muon did not fire the Level-1 trigger; *line histogram:* test muon did fire the Level-1 trigger.

The dominant experimental systematic uncertainties on $\sigma_Z \cdot \mathrm{Br}(Z \to \mu^+\mu^-)$ arise from the limited size of the Z data sample currently available to make such efficiency measurements ($\pm$ 3.3%) and from PDF's ($\pm$ 1.6%). The preliminary result is:

$$\sigma_Z \cdot \mathrm{Br}(Z \to \mu^+\mu^-) = 261.8 \pm 5.0(\mathrm{stat.}) \pm 8.9(\mathrm{syst.}) \pm 26.2(\mathrm{lum.})\ \mathrm{pb}.$$

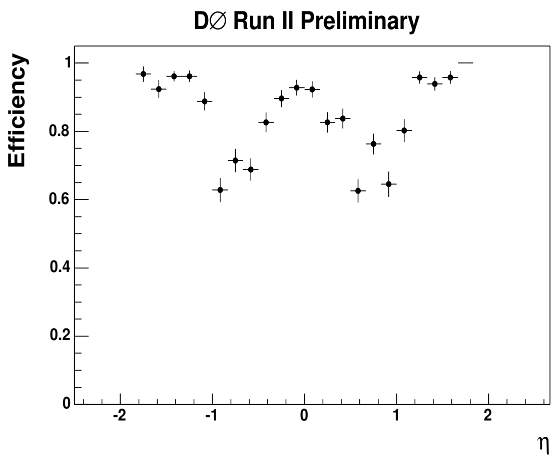

Figure 7. Efficiency per muon of the DØ Level-1 muon trigger as a function of η.

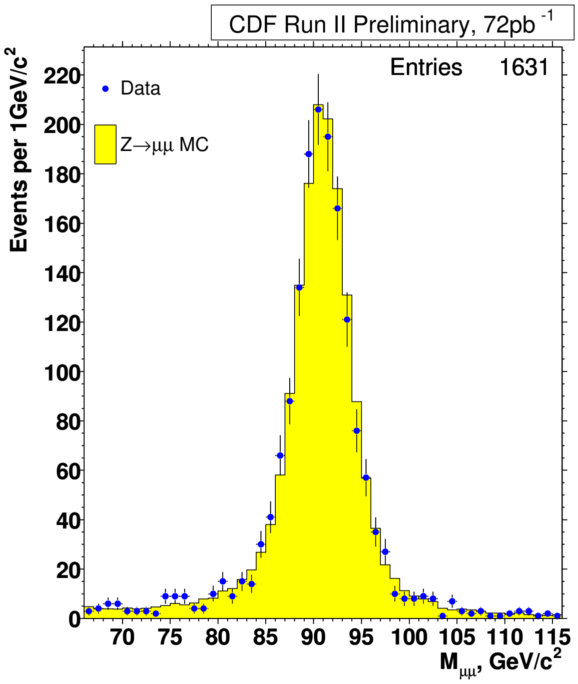

Figure 8. The invariant mass of CDF $\mu^+\mu^-$ candidates.

1.3. *CDF: $Z \to \mu^+\mu^-$*

All of the CDF measurements of $\sigma \cdot \mathrm{Br}$ for Z and W at this conference correspond to $\int L = 72$ pb^{-1}. The event selection cuts for $Z \to \mu^+\mu^-$ require two oppositely charged central tracks that are identified as muons and have $p_T > 20$ GeV. Both of the muons are required to be isolated. Events are selected over a fairly restricted angular range: at least one muon is required to satisfy $|\eta| < 0.6$ and both muons are required to satisfy $|\eta| < 1.0$. A cut on the invariant mass of the $\mu^+\mu^-$ system around the Z mass is made: $66 < \mathrm{M}_{\mu\mu} < 116$ GeV. The total acceptance $\times$ efficiency for a $Z \to \mu^+\mu^-$ event to be triggered and selected is 9% and the candidate event sample comprises 1631 events. The invariant mass of the CDF $\mu^+\mu^-$ candidates is shown in Fig. 8. The dominant backgrounds arise from cosmic ray muons $(0.9 \pm 0.9)\%$. The largest experimental systematic uncertainty arises from PDF's ($\pm$ 3%); this is larger than for the corresponding DØ analysis due to the more restricted angular acceptance of the CDF event selection. The preliminary result is:

$$\sigma_Z \cdot \mathrm{Br}(Z \to \mu^+\mu^-) = 246 \pm 6(\mathrm{stat.}) \pm 12(\mathrm{syst.}) \pm 15(\mathrm{lum.})\ \mathrm{pb}.$$

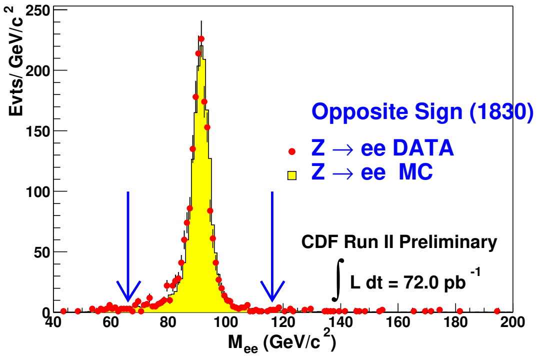

Figure 9. The invariant mass of CDF e^+e^- candidates.

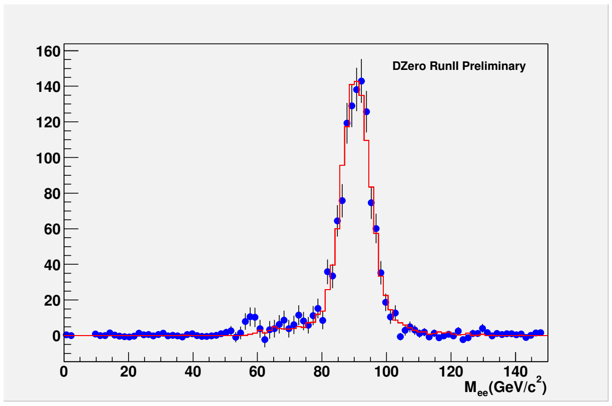

Figure 10. The invariant mass of DØ e^+e^- data *(points with error bars)* compared to Monte Carlo *(line histogram)*.

1.4. *CDF and DØ: $Z \to e^+e^-$*

CDF and DØ employ very similar cuts to select candidate $Z \to e^+e^-$ events: two isolated electron candidates are required with $\mathrm{E_T} > 25$ GeV and $|\eta| < 1.1$. The invariant mass of the 1830 CDF e^+e^- candidates is shown in Fig. 9. The CDF result is:

$$\sigma_Z \cdot \mathrm{Br}(Z \to e^+e^-) = 267.0 \pm 6.3(\mathrm{stat.}) \pm 15.2(\mathrm{syst.}) \pm 16.0(\mathrm{lum.})\ \mathrm{pb}.$$

The invariant mass of the 1631 DØ e^+e^- candidates from $\int L = 42$ pb^{-1} is shown in Fig. 10. The DØ result is:

$$\sigma_Z \cdot \mathrm{Br}(Z \to e^+e^-) = 275 \pm 9(\mathrm{stat.}) \pm 9(\mathrm{syst.}) \pm 28(\mathrm{lum.})\ \mathrm{pb}.$$

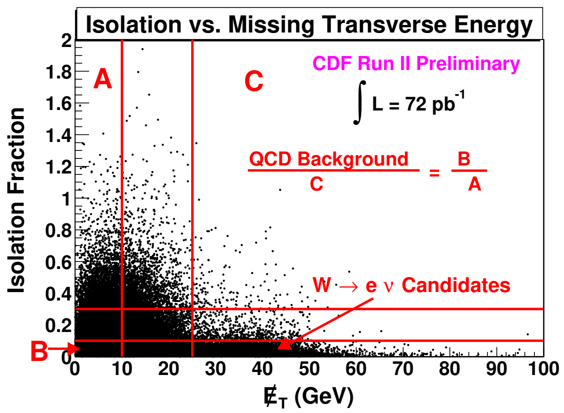

Figure 11. CDF electron data: the degree to which the electron is isolated vs. E_T^{miss}.

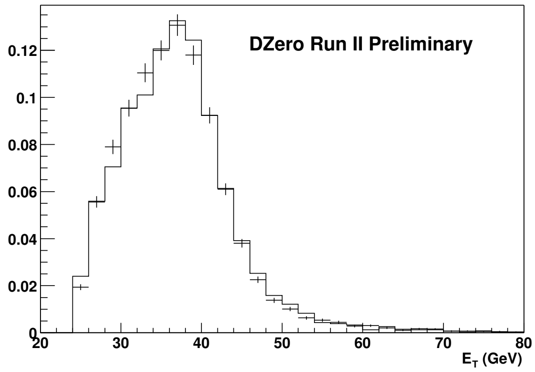

Figure 12. The electron E_T distribution in DØ $W \to e\nu$ data *(points with error bars)* compared to Monte Carlo *(line histogram)*.

1.5. *CDF and DØ: $W \to e\nu$*

In selecting candidate $W \to e\nu$ events both CDF and DØ require an isolated electron candidate with $E_T > 25$ GeV and $E_T^{miss} > 25$ GeV. The background to $W \to \ell\nu$ is dominated by QCD events in which a jet fakes the isolated lepton signal. Monte Carlos cannot be trusted to provide an adequate description of the background processes and so the level of background is estimated using the data. A method used to estimate the background is illustrated by Fig. 11, which shows for the CDF electron data the degree to which the electron is isolated vs. E_T^{miss}. The candidate $W \to e\nu$ events occupy the lower right area of the plot, which corresponds to isolated electrons and high E_T^{miss}. The rest of the plot is dominated by background. The probability for the electron candidate in a background event to appear to be isolated is estimated by taking the ratio of the numbers of events in regions A and B in Fig. 11, which are both at low E_T^{miss}. The number of background events in the signal region is estimated by applying this factor to the number of non-isolated events with high E_T^{miss} (region C). The accuracy of this method is limited by kinematic correlations between isolation and E_T^{miss} for the background events. CDF quotes an estimated background of (3.5 ±1.7)%; the 50% uncertainty is evaluated by making large variations in the boundaries of the regions A, B and C and seeing by how much the estimated background changes. With 38628 candidate $W \to e\nu$ events the CDF result is:

$$\sigma_W \cdot \mathrm{Br}(W \to e\nu) = 2.64 \pm 0.01(\mathrm{stat.}) \pm 0.09(\mathrm{syst.}) \pm 0.16(\mathrm{lum.})\ \mathrm{nb}.$$

Figure 12 shows the electron E_T distribution in DØ $W \to e\nu$ data *(points with error bars)* compared to Monte Carlo *(line histogram)*. 27370 events are selected from $\int L = 42$ pb^{-1} and the result is:

$$\sigma_W \cdot \mathrm{Br}(W \to e\nu) = 2.88 \pm 0.02(\mathrm{stat.}) \pm 0.13(\mathrm{syst.}) \pm 0.29(\mathrm{lum.})\ \mathrm{nb}.$$

1.6. *CDF and DØ: $W \to \mu\nu$*

In selecting candidate $W \to \mu\nu$ events both CDF and DØ require an isolated muon candidate with $p_T > 20$ GeV and $E_T^{miss} > 20$ GeV. At present, the background to $W \to \mu\nu$ for both experiments has a large contribution from $Z \to \mu^+\mu^-$ events in which one of the muons is not reconstructed, as well as from QCD events in which a muon in a jet fakes the isolated muon signal.

The "transverse mass", M_T, is given by:

$$M_T = \sqrt{2 p_T E_T^{miss}(1 - \cos\Delta\phi)},$$

where $\Delta\phi$ is the difference in azimuthal angle between the p_T of the charged lepton candidate and the missing transverse momentum vector. M_T corresponds to the invariant mass of the muon-neutrino system, taking only their momentum components in the plane perpendicular to the beam direction into account. Figure 13 shows the M_T of CDF $W \to \mu\nu$ candidates. The total background is estimated to be (10.8 ± 1.1)%, the number of candidate events is 21599 and the result is:

$$\sigma_W \cdot \mathrm{Br}(W \to \mu\nu) = 2.64 \pm 0.02(\mathrm{stat.}) \pm 0.12(\mathrm{syst.}) \pm 0.16(\mathrm{lum.})\ \mathrm{nb}.$$

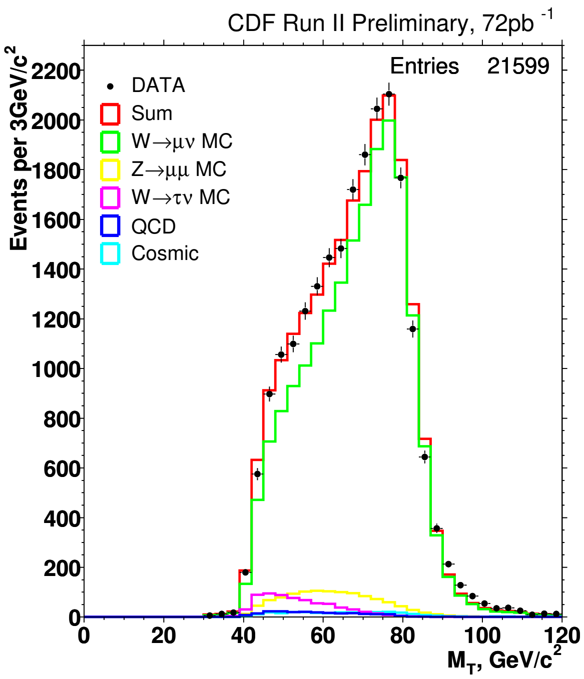

Figure 13. The M_T of CDF $W \to \mu\nu$ candidates.

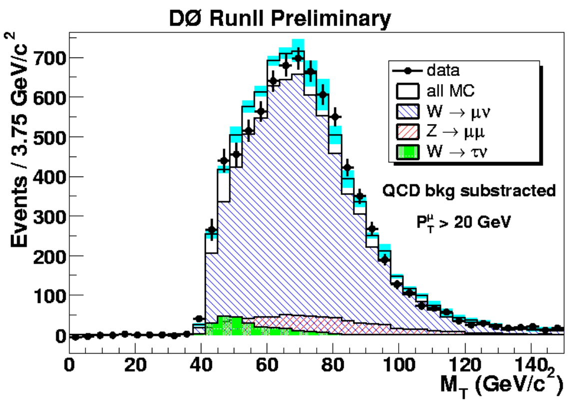

Figure 14. The M_T of DØ $W \to \mu\nu$ candidates.

Figure 14 shows the M_T of DØ $W \to \mu\nu$ candidates. The total background is estimated to be $(11.4 \pm 1.8)\%$, the number of candidate events is 7352 from $\int L = 17\ \mathrm{pb}^{-1}$ and the result is:

$$\sigma_W \cdot \mathrm{Br}(W \to \mu\nu) = 3.23 \pm 0.13(\mathrm{stat.}) \pm 0.10(\mathrm{syst.}) \pm 0.32(\mathrm{lum.})\ \mathrm{nb}.$$

1.7. *CDF: $W \to \tau\nu$*

CDF selects candidate hadronic tau decays by looking for a narrow jet that is contained within a cone of half-width 10° and is isolated within a wider cone of half-width 30°. Candidate $W \to \tau\nu$ events are selected by requiring $p_T > 25$ GeV for the hadronic tau candidate and $E_T^{\mathrm{miss}} > 25$ GeV. The estimated contributions to the selected sample of 2345 events are illustrated in Fig. 15, which shows the number of charged tracks associated with the tau candidates. The result is:

$$\sigma_W \cdot \mathrm{Br}(W \to \tau\nu) = 2.67 \pm 0.07(\mathrm{stat.}) \pm 0.21(\mathrm{syst.}) \pm 0.16(\mathrm{lum.})\ \mathrm{nb}.$$

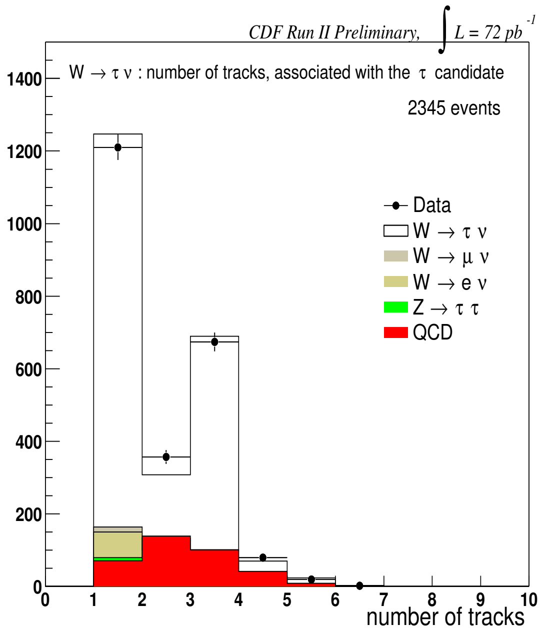

Figure 15. The number of charged tracks associated with CDF $W \to \tau\nu$ candidates.

2. Combination of $\sigma \cdot$ Br Results from CDF and DØ

2.1. *Luminosity Determination*

CDF and DØ determine the delivered luminosity by measuring the total rate of inelastic $p\bar{p}$ collisions. The luminosity determination therefore requires knowledge of the total inelastic cross section, $\sigma_{\mathrm{inelastic}}$. This cross section has been measured during Tevatron Run I at $\sqrt{s} = 1.8$ TeV by two experiments: CDF and E811. These two measurements disagree at the level of three standard deviations. There is some ambiguity as to how to perform an average of these two inconsistent values – different methods lead to results in the range $59.1 < \sigma_{\rm inelastic} < 60.7$ mb (2.7% difference) when extrapolated to $\sqrt{s} = 1.96$ TeV.

For the $\sigma \cdot$ Br results reported in the preceding sections CDF uses $\sigma_{\rm inelastic} = 60.7$ mb and DØ uses $\sigma_{\rm inelastic} = 57.6$ mb (which corresponds to a 5.3% difference). For the combinations presented below I have chosen[a] to:

- scale the reported $\sigma \cdot$ Br values to correspond to a consistent value of $\sigma_{\rm inelastic}$.
  - I have chosen: $\sigma_{\rm inelastic} = 60.7$ mb, the value used by CDF.
  - This choice corresponds to multiplying the DØ $\sigma \cdot$ Br values reported in the preceding sections by a factor 1.053.
- quote an additional 2.7% systematic error to cover the ambiguity in the choice of $\sigma_{\rm inelastic}$. This leads to a total error of $(4.0 \oplus 2.7 = 4.8)\%$ assumed for $\sigma_{\rm inelastic}$, which is 100% correlated between CDF and DØ.

2.2. *Combined $\sigma \cdot$ Br Results*

The $\sigma \cdot$ Br values given in Sec. 1 have been combined. The luminosity scale and uncertainty are treated as described in Sec. 2.1. At the present level of accuracy the only other source of systematic uncertainty that introduces significant correlations among the measurements arises from the PDF's.

Figure 16 shows the resulting combined CDF and DØ measurement of $\sigma_Z \cdot {\rm Br}(Z \to \ell^+\ell^-)$:

$$\sigma_Z \cdot {\rm Br}(Z \to \ell^+\ell^-) = 258 \pm 10({\rm expt.}) \pm 16({\rm lum.})\ {\rm pb}.$$

Also shown are the individual CDF and DØ measurements of $\sigma_Z \cdot {\rm Br}(Z \to \mu^+\mu^-)$ and $\sigma_Z \cdot {\rm Br}(Z \to e^+e^-)$. These values are compared to the Standard Model NNLO expectation:[2]

$$\sigma_Z \cdot {\rm Br}(Z \to \ell^+\ell^-) = 252 \pm 9\ {\rm pb}.$$

[a]These issues have been discussed within the Tevatron Electroweak Working Group (TeVEWWG), but no official policy has yet been agreed by CDF and DØ. The results given below labelled as "my combination" should be taken as the responsibility of this review speaker and not officially sanctioned CDF/DØ results.

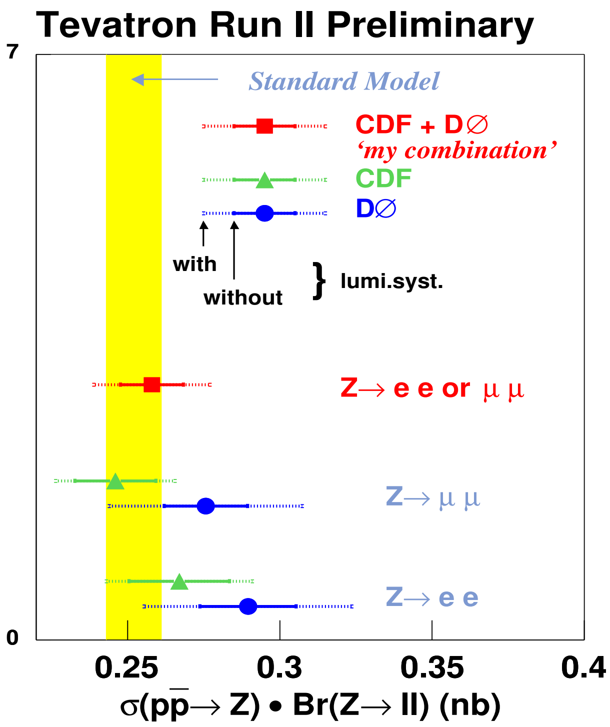

Figure 16. Combined CDF and DØ measurement of $\sigma_Z \cdot {\rm Br}(Z \to \ell^+\ell^-)$ compared with the Standard Model expectation. Also shown are the individual measurements of $\sigma_Z \cdot {\rm Br}(Z \to \mu^+\mu^-)$ and $\sigma_Z \cdot {\rm Br}(Z \to e^+e^-)$.

Figure 17 shows the combined CDF and DØ measurement of $\sigma_W \cdot {\rm Br}(W \to \ell\nu)$:

$$\sigma_W \cdot {\rm Br}(W \to \ell\nu) = 2.69 \pm 0.09({\rm expt.}) \pm 0.17({\rm lum.})\ {\rm nb}.$$

Also shown are the individual CDF and DØ measurements of $\sigma_W \cdot {\rm Br}(W \to \mu\nu)$ and $\sigma_W \cdot {\rm Br}(W \to e\nu)$. These values are compared to the Standard Model NNLO expectation:[2]

$$\sigma_W \cdot {\rm Br}(W \to \ell\nu) = 2.72 \pm 0.10\ {\rm pb}.$$

In the Tevatron combined $\sigma \cdot$ Br measurements for both Z and W, the experimental (non lumi.) error is dominated by uncertainties of a statistical nature.

2.3. *Quantities Derived from the Combined $\sigma \cdot$ Br Results*

A number of interesting quantities may be derived from the above $\sigma \cdot$ Br results. It is useful to define the ratio of the $\sigma \cdot$ Br values for W and Z:

$$R_\ell = \frac{\sigma_W \cdot {\rm Br}(W \to \ell\nu)}{\sigma_Z \cdot {\rm Br}(Z \to \ell^+\ell^-)}.$$

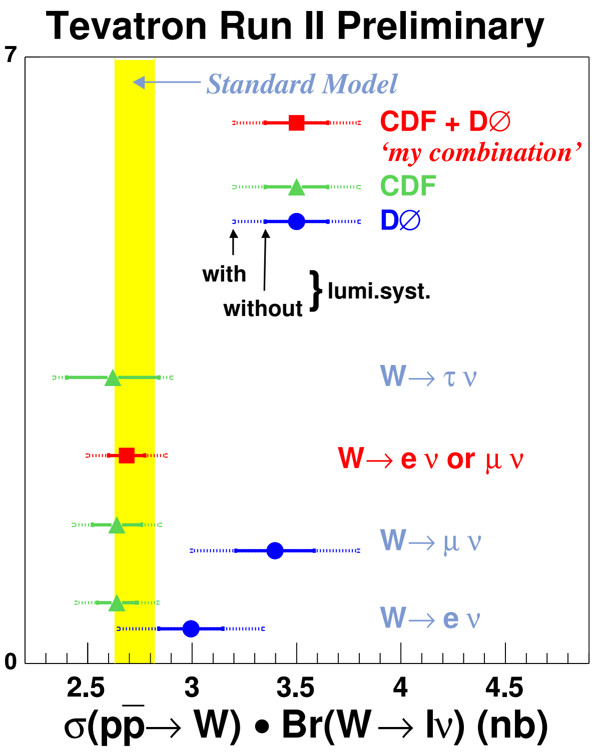

Figure 17. Combined CDF and DØ measurement of $\sigma_W \cdot \mathrm{Br}(W \to \ell\nu)$ compared with the Standard Model expectation. Also shown are the individual measurements of $\sigma_W \cdot \mathrm{Br}(W \to \mu\nu)$ and $\sigma_W \cdot \mathrm{Br}(W \to e\nu)$.

In taking this ratio the luminosity uncertainties cancel and other important systematic uncertainties partially cancel, for example, those arising from PDF's and the efficiencies to trigger and select high p_T, isolated leptons. The Tevatron Electroweak Working Group (TeVEWWG) has evaluated the correlated systematic uncertainties and has previously averaged the CDF electron and muon and the DØ electron results.[4] For this conference the value of R_ℓ has been updated[b] to include a value of R_ℓ extracted[c] from the DØ muon results: $\mathrm{R}_\mu = 12.32 \pm 0.73$. Figure 18 shows the updated combined CDF and DØ measurement of R_ℓ from Run II:

$$\mathrm{R}_\ell = 10.61 \pm 0.30,$$

which when combined with the values from Run I yields the value:

$$\mathrm{R}_\ell = 10.59 \pm 0.20.$$

As can be seen in the figure, these results are in agreement the Standard Model expectation.

The value of R_ℓ can be used to make an indirect determination of the leptonic branching ratio of the W, $\mathrm{Br}(W \to \ell\nu)$. This follows from the definition of R_ℓ given above, with the ratio of the W and Z production cross sections input from a NNLO calculation and the value of $\mathrm{Br}(Z \to \ell^+\ell^-)$ as measured at LEP. Figure 19 shows the values of $\mathrm{Br}(W \to e\nu)$, $\mathrm{Br}(W \to \mu\nu)$ and $\mathrm{Br}(W \to \ell\nu)$ extracted from the Tevatron-combined values of R given in Fig. 18. These results are compared with the measurements made at LEP and with the Standard Model expectation.

The W leptonic branching ratio may be expressed as:

$$\mathrm{Br}(W \to \ell\nu) = \Gamma(W \to \ell\nu)/\Gamma_\mathrm{W}.$$

Since the W leptonic partial width, $\Gamma(W \to \ell\nu)$, can be predicted very accurately within the SM, $\mathrm{Br}(W \to \ell\nu)$ may thus be interpreted as an indirect measurement of the W total width, Γ_W. The Tevatron combined Run I plus Run II indirect measurement using this technique is[d]:

$$\Gamma_\mathrm{W} = 2.135 \pm 0.053 \text{ GeV}.$$

This may be compared with the direct measurement of Γ_W from the W lineshape, combining LEP plus the Tevatron Run I, of:

$$\Gamma_\mathrm{W} = 2.139 \pm 0.069 \text{ GeV}.$$

2.4. *Future Prospects*

There is a promising future for further improvements in the accuracy of such "ratio" measurements at the Tevatron. Although at present the $\mathrm{Br}(W \to \ell\nu)$ measurements from LEP are the most accurate available, these measurements are limited in precision by the statistical uncertainties from samples of only $O(10^3)$ leptonic W decays per channel and per experiment. With a dataset of $O(1\ \mathrm{fb}^{-1})$ within the next couple of years at the Tevatron we expect to select

[b] The updated combination follows exactly the method used previously by TeVEWWG. However, since there was insufficient time for this new combination to pass through the official approval procedures of the collaborations it should be regarded as the responsibility of the speaker.
[c] "my combination"

[d] "my combination"

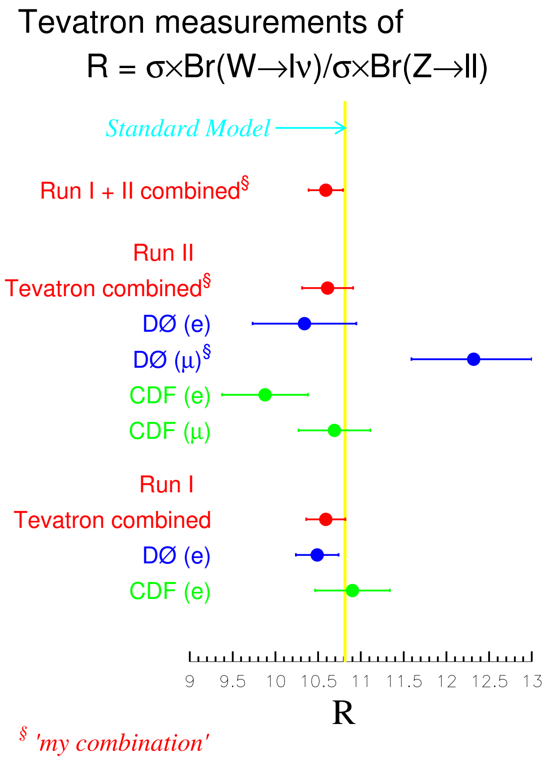

Figure 18. Combined CDF and DØ measurement of R_ℓ from Run II and Run I compared with the Standard Model expectation. Also shown are the individual measurements of R_ℓ in the electron and muon channels.

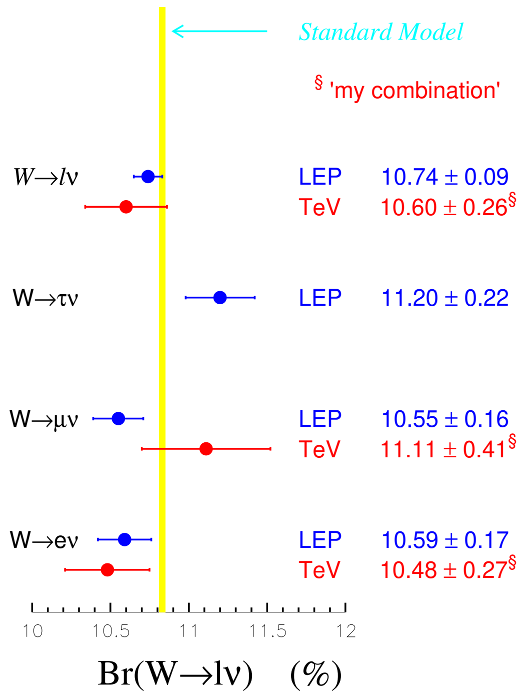

Figure 19. Measurements of $\mathrm{Br}(W \to \ell\nu)$ from LEP and the Tevatron compared with the Standard Model expectation.

$O(10^6)$ $W \to \ell\nu$ events per channel and per experiment. It will, of course, be a considerable challenge to beat systematic uncertainties down to the few per mille level to keep pace with the statistical errors. However, the samples of $O(10^5)$ $Z \to \ell^+\ell^-$ events that are expected per channel and per experiment will play a large part in achieving the precise systematic understanding of detector performance and phenomenology that will be necessary. In addition, considerable skill will be needed to design and implement experimental triggers and event selections with sufficient redundancy to achieve the necessary precision.

In parallel to the expected increase in experimental precision, much theoretical progress is currently being made in understanding, for example, NNLO cross section calculations and PDF's, and in quantifying PDF uncertainties. This should allow the production cross sections of W and Z to be predicted at the level of about 1% and their ratio at the level of few per mille.[5] This offers the prospect that the experimental luminosity for the rest of the Tevatron physics programme could be determined with a better precision than can ever be expected from the luminosity determinations based on the total rate of inelastic collisions.

3. Other Measurements with Events Containing W and Z Bosons

With sizeable samples of W and Z events now becoming available, many other interesting measurements are starting to be made. Studies sensitive to possible new physics include measurements of the high mass tail of the $\ell^+\ell^-$ invariant mass distribution (see Figs. 20 and 21) and the forward-backward charge asymmetry of $\ell^+\ell^-$ events (see Fig. 22).

Understanding the QCD phenomenology of IVB production is an important part of the physics programme with W and Z events. This is of interest both as a topic in its own right and also because

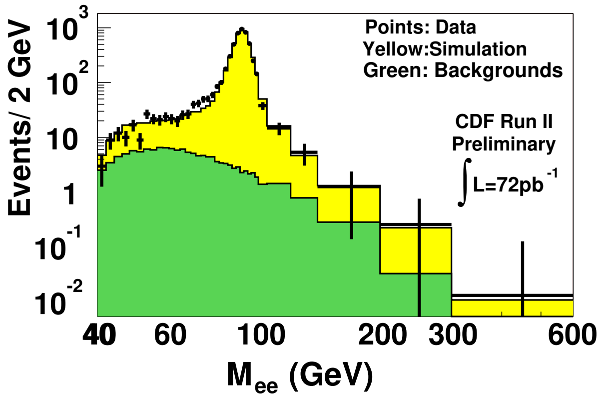

Figure 20. The invariant mass of CDF e^+e^- candidates showing the high mass region.

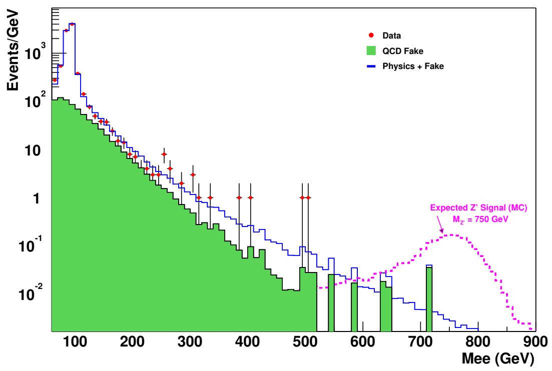

Figure 21. The invariant mass of DØ e^+e^- candidates showing the high mass region.

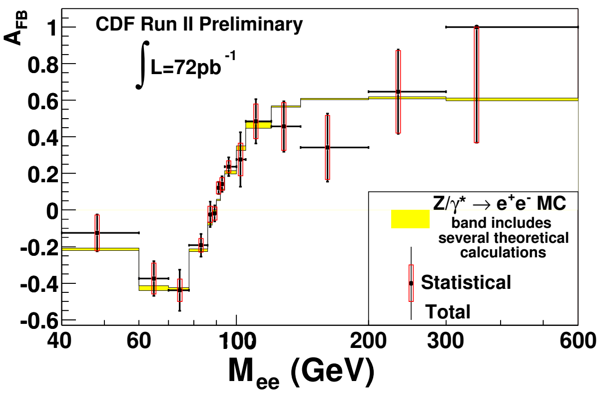

Figure 22. The A_{fb} of CDF e^+e^- candidates as a function of the e^+e^- invariant mass.

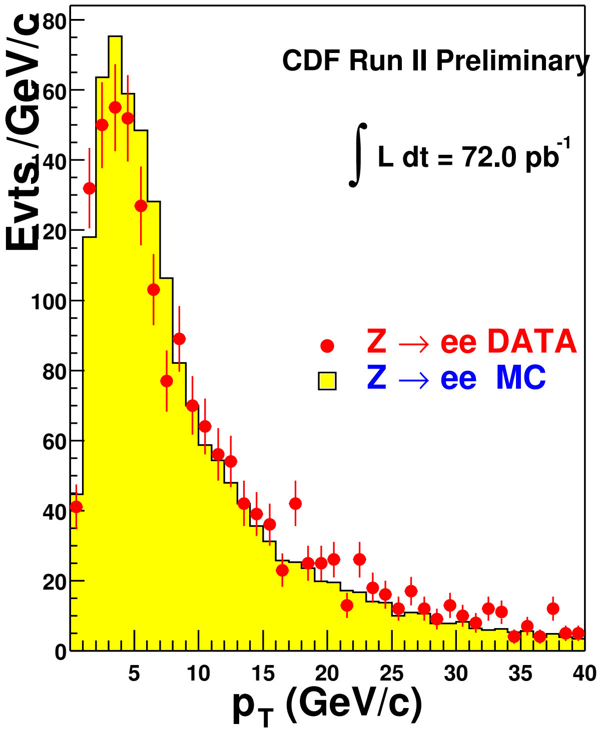

Figure 23. The p_T of CDF e^+e^- candidates.

a precise understanding of this phenomenology and the degree to which QCD Monte Carlos describe the data will be necessary to control systematic uncertainties in much of the physics programme at CDF and DØ (e.g. measuring the W and top masses). As an example of first steps in this direction, Figs. 23 and 24 show the p_T of e^+e^- candidates in CDF and $\mu^+\mu^-$ candidates in DØ, respectively, compared to Monte Carlo simulations. Other measurements that probe PDF's and QCD phenomenology that can be expected in the future include: the rapidity distribution of Z's, the p_T distribution of W's, and the charge asymmetry in $W \to \ell\nu$ events.

4. Selection of Events Containing Two Electroweak Bosons

The selection of events containing two electroweak IVB's are of interest, for example, because they allow measurements of the self-coupling of the IVB's and they allow searches to be made for new particles or interactions. The SM cross sections for events con-

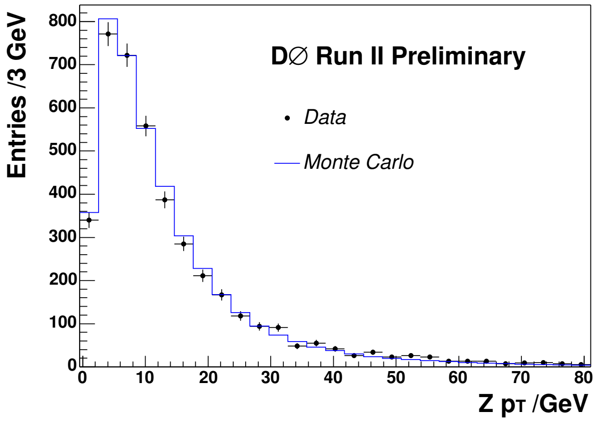

Figure 24. The p_T of DØ $\mu^+\mu^-$ candidates.

taining two electroweak IVB's are very small and so only small samples of such events are expected with the present datasets. However, CDF has updated its results in this area with samples that correspond to $\int L$ of around 126 pb^{-1}, and this promises to be an area of considerable activity in the future.

4.1. $Z\gamma$ and $W\gamma$

CDF selects $Z\gamma$ and $W\gamma$ events by requiring, in addition to the standard Z and W event selections, the presence of a central photon candidate with $\mathrm{E_T} > 7$ GeV that is spatially separated from the charged lepton(s) in the event according to:

$$\Delta\mathrm{R} = \sqrt{\Delta\phi^2 + \Delta\eta^2} > 0.7,$$

where $\Delta\phi$ and $\Delta\eta$ are the separation in azimuthal angle and pseudo-rapidity between the photon and the nearest charged lepton. Figure 25 shows the invariant mass of the $\ell^+\ell^-\gamma$ system vs. the invariant mass of the $\ell^+\ell^-$ system for CDF $Z\gamma$ candidates. The concentration of 3-body masses at $\mathrm{M_Z}$ seen in the Monte Carlo events is due to final-state radiation from one of the charged leptons. The concentration of 2-body masses at $\mathrm{M_Z}$ is due to initial-state radiation. 47 events are observed as compared with 43 events expected. CDF quotes a $\sigma \cdot \mathrm{Br}$ value for $Z \to \ell^+\ell^-$ containing a photon satisfying the above kinematic cuts on $\mathrm{E_T}$ and $\Delta\mathrm{R}$:

$$\sigma \cdot \mathrm{Br} = 5.8 \pm 1.0(\mathrm{stat.}) \pm 0.4(\mathrm{syst.}) \pm 0.4(\mathrm{lum.})\ \mathrm{pb}.$$

Figure 26 shows the $\mathrm{M_T}$ of the $\ell\nu\gamma$ system vs. the $\mathrm{M_T}$ of the $\ell\nu$ system for CDF $W\gamma$ candidates. 133

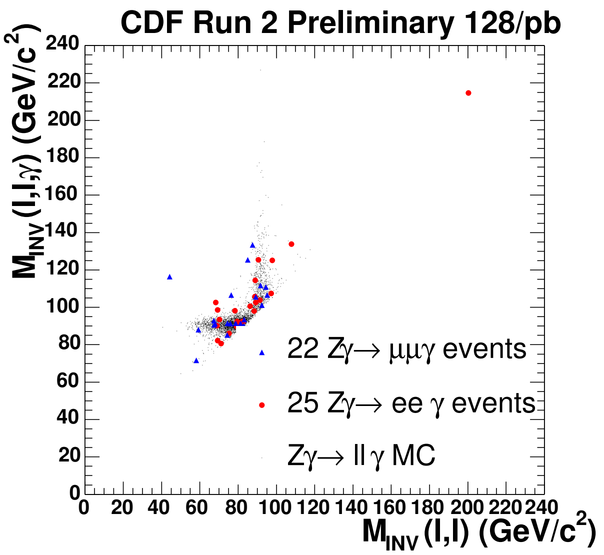

Figure 25. Invariant mass of $\ell^+\ell^-\gamma$ system vs. invariant mass of $\ell^+\ell^-$ system for CDF $Z\gamma$ candidates.

events are observed as compared with 141 events expected. CDF quotes a $\sigma \cdot \mathrm{Br}$ value for $W \to \ell\nu$ containing a photon satisfying the above kinematic cuts on $\mathrm{E_T}$ and $\Delta\mathrm{R}$:

$$\sigma \cdot \mathrm{Br} = 17.2 \pm 2.2(\mathrm{stat.}) \pm 2.0(\mathrm{syst.}) \pm 1.2(\mathrm{lum.})\ \mathrm{pb}.$$

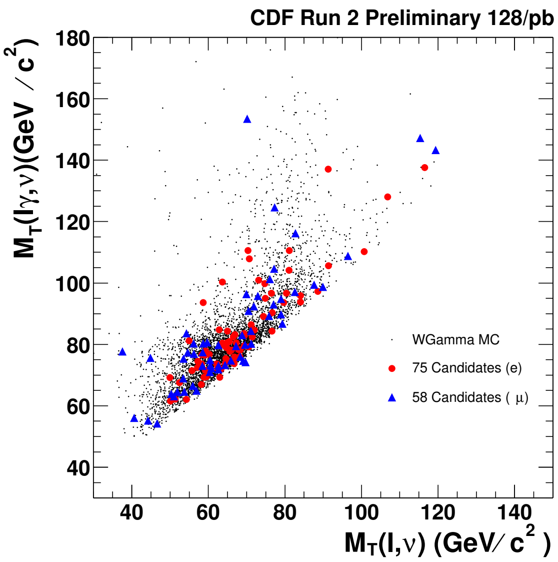

Figure 26. $\mathrm{M_T}$ of $\ell\nu\gamma$ vs. $\mathrm{M_T}$ of $\ell\nu$ for CDF $W\gamma$ candidates.

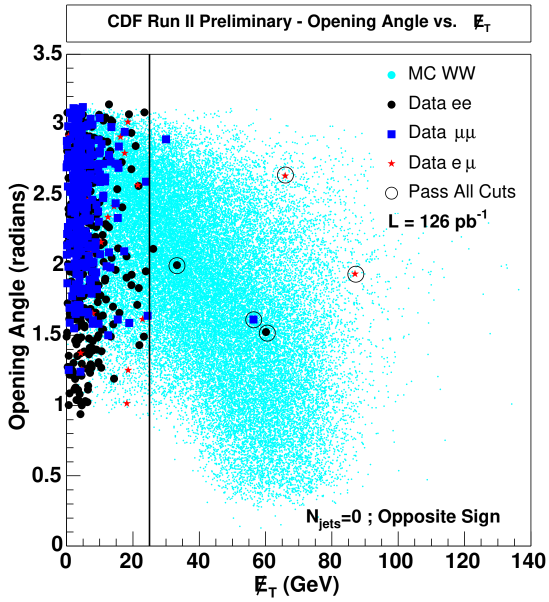

Figure 27. CDF WW selection: the opening angle between the two leptons vs. $\mathrm{E_T^{miss}}$. The 5 selected signal events are indicated as points within a circle.

4.2. *WW Search*

CDF has performed a search for WW events in the channels e^+e^-, $\mu^+\mu^-$ and $e^\pm\mu^\mp$. A pair of oppositely charged, isolated, high p_T lepton candidates is required in events with high $\mathrm{E_T^{miss}}$. In the e^+e^- and $\mu^+\mu^-$ channels, events are removed if the lepton pair mass is consistent with $\mathrm{M_Z}$. Events containing hadronic jets are removed. Figure 27 shows the opening angle between the two leptons vs. $\mathrm{E_T^{miss}}$. 5 signal events are selected, to be compared with 9.2 events expected, of which 2.3 are background and 6.9 are signal. Clearly, it is too early to claim observation of WW in Run II.

4.3. *Summary*

Analyses of events containing W and Z are now becoming available from CDF and DØ with datasets from Run II corresponding to $\int L$ of around 120 pb^{-1} – well in excess of the $\int L$ collected in Run I. So far, these analyses have concentrated on selection of the event samples and measuring the relevant cross section times branching ratios. The detailed understanding of the performance of the detectors, triggers, event reconstruction algorithms, calibrations, and Monte Carlos required by such measurements benefits the entire physics programmes of the two experiments. Detailed measurements of the properties of the selected events have started and should lead to interesting results in the near future.

It is in the interests of the two Tevatron experiments and Fermilab that prompt and authoritative combinations of the latest results from CDF and DØ are provided. I hope that I am the last review speaker at a major international conference who has to present combinations of Tevatron results with the proviso "my combination". Clearly the individual experiments have complete responsibility for deciding which of their results are released into the public domain. In addition, the *procedures* for combining results from the two experiments have to be subjected to the full scrutiny of internal collaboration review. However, once this has occurred I hope that in future any *particular combination of the latest set of results* can be performed by the TeVEWWG and presented in public without the need for an additional protracted period of internal review by the individual collaborations.

Acknowledgments

I am grateful to the CDF and DØ collaborations for providing me with their preliminary results and descriptions of the associated analyses. I thank the other members of the Tevatron Electroweak Working Group for useful discussions and for establishing the procedures used to combine the values of R_ℓ, $\mathrm{Br}(W \to \ell\nu)$ and Γ_W: Sarah Eno, Harald Fox, Martin Grünewald, Eva Halkiadakis, Eric James, Ashutosh Kotwal, Giulia Manca, Sean Mattingly, Pasha Murat, Emily Nurse, Michael Schmitt, Georg Steinbrück, Paul Telford, Alexei Varganov, Marco Verzocchi, and Junjie Zhu. In particular, I thank Martin Grünewald for his invaluable help in making the combinations given in Sec. 2; they should perhaps more properly have been labelled "our combination". I am grateful to Martin Grünewald and Emily Nurse for their useful comments on a draft version of this note.

I gratefully acknowledge support from the UK Particle Physics and Astronomy Research Council in the form of a PPARC Senior Research Fellowship.

References

1. J. Pumplin *et al.*, hep-ph/0201195.
2. The Standard Model NNLO expected $\sigma \cdot \mathrm{Br}$ values are calculated using: R. Hamberg *et al.*, *Nucl. Phys.* B **359**, 1991 (343). The central value uses the MRST2002 NNLO PDF's.[3] The 3.5% uncertainty is assessed using the CTEQ6 error PDF's. The LEP value $\mathrm{Br}(Z \to \ell^+\ell^-) = 0.03366 \pm 0.00002$ and the SM value $\mathrm{Br}(W \to \ell\nu) = 0.1082 \pm 0.0002$ are used.
3. A. D. Martin *et al.*, hep-ph/0211080.
4. The Tevatron Electroweak Working Group, http://tevewwg.fnal.gov/wz/eps2003/
5. See, for example, the talk by Robert Thorne in these proceedings.

DISCUSSION

Rohini Godbole (Indian Institute of Science, Bangalore): What is the expected error on the $\mathrm{M_W}$ measurement now that the upgraded detectors are in operation, and how does it compare with the 30 MeV given in the studies made before Run II started?

Terry Wyatt: The description of the data by the Monte Carlos is adequate for the purposes of estimating event selection efficiencies and backgrounds in the $\sigma \cdot \mathrm{Br}$ measurements presented here. However, as I mentioned in my talk already, at the level of detail needed for $\mathrm{M_W}$ measurements there are considerable disagreements (see, for example, Figs. 12 and 13). A great deal of careful work to understand detector performance and phenomenology will be needed before $\mathrm{M_W}$ measurements with the current data will be feasible. At present there is not much one can say beyond the estimates made before Run II of around 30 MeV.

Thomas Gehrmann (Zurich Univ.): You briefly mentioned the option of using W and Z cross sections to determine the luminosity of the Tevatron. What are the actual prospects for this to become the default luminosity calibration?

Terry Wyatt: From the experimental point of view I am very confident that we shall understand efficiencies and backgrounds for $Z \to \ell^+\ell^-$ and $W \to \ell\nu$ selections at the level of better than 1%. As I also mentioned, there is currently a lot of theoretical activity that should allow the production cross sections of W and Z to be predicted at the level of about 1%.[5] Therefore, there is every likelihood that the *overall* luminosity scale for the general physics programme will be set by measuring the numbers of observed $Z \to \ell^+\ell^-$ and $W \to \ell\nu$ events. Of course, we still need as precise as possible measurements of the total rate of inelastic collisions and knowledge of $\sigma_{\mathrm{inelastic}}$. Measurements of the total inelastic rate will certainly be needed for measurement of *relative* luminosities, minute by minute and run by run. They are also essential for the kind of detailed book-keeping and stability checks needed for precision measurements. In addition, we should like to test the predictions for the Z and W production cross sections by having an alternative absolute luminosity measurement (albeit with an accuracy likely to be limited at the level of about 5%).

Un-Ki Yang (Univ. of Chicago): The DØ measurement of $\mathrm{R}_\mu = \dfrac{\sigma_{\mathrm{W}} \cdot \mathrm{Br}(W \to \mu\nu)}{\sigma_{\mathrm{Z}} \cdot \mathrm{Br}(Z \to \mu^+\mu^-)}$ seems a little high, because of a high $\sigma_{\mathrm{W}} \cdot \mathrm{Br}(W \to \mu\nu)$. In CDF we learned that there are many high p_{T} muons from low p_{T} kaon decays inside the tracking volume. I wonder how this background is removed.

Terry Wyatt: Firstly, the value of R_μ from DØ is not inconsistent with the other measured values of R_ℓ. A Kolmogorov-Smirnov test gives a 20% probability for consistency of the set of R_ℓ measurements. Secondly, the level of background from pion and kaon decay in flight is very small in DØ due to the small radius of the tracking detectors. We'd expect the methods used to evaluate QCD backgrounds to the $W \to \mu\nu$ sample to take any residual background into account.